POLITECNICO DI TORINO
Repository ISTITUZIONALE

Vectorized Thrust Measurement for Aerospace Propulsion Nozzles

*Original*
Vectorized Thrust Measurement for Aerospace Propulsion Nozzles / Hassan, J., Di Cicca, G.M., Ferlauto, M., Marsilio, R.. - ELETTRONICO. - (2025), pp. 734-738. (IEEE MetroAeroSpace 2025 Naples (ITA) 18-20 June, 2025) [10.1109/MetroAeroSpace64938.2025.11114490].

*Availability:*
This version is available at: 11583/3001969 since: 2025-07-20T15:43:50Z

*Publisher:*
IEEE

*Published*
DOI:10.1109/MetroAeroSpace64938.2025.11114490

*Terms of use:*

This article is made available under terms and conditions as specified in the corresponding bibliographic description in the repository

*Publisher copyright*
IEEE postprint/Author's Accepted Manuscript

©2025 IEEE. Personal use of this material is permitted. Permission from IEEE must be obtained for all other uses, in any current or future media, including reprinting/republishing this material for advertising or promotional purposes, creating new collecting works, for resale or lists, or reuse of any copyrighted component of this work in other works.

(Article begins on next page)

20 November 2026

# Vectorized Thrust Measurement for Aerospace Propulsion Nozzles

Jehangir Hassan
*Department of Mechanical and Aerospace Engineering*
*Politecnico di Torino*
Turin, Italy
jehangir.hassan@polito.it

Gaetano Maria Di Cicca
*Department of Mechanical and Aerospace Engineering*
*Politecnico di Torino*
Turin, Italy
gaetano.dicicca@polito.it

Michele Ferlauto
*Department of Mechanical and Aerospace Engineering*
*Politecnico di Torino*
Turin, Italy
michele.ferlauto@polito.it

Roberto Marsilio
*Department of Mechanical and Aerospace Engineering*
*Politecnico di Torino*
Turin, Italy
roberto.marsilio@polito.it

***Abstract*—This paper presents a measurement system for assessing the thrust produced by advanced aerospace propulsion nozzles. The system is able to evaluate the transverse components of thrust in the case of vectorized nozzles using three precision balances positioned at the base of the test rig. The balances are arranged in a 120-degree configuration to accurately reconstruct the thrust vector. Cold flow experiments using air as the working fluid are carried out for a linear aerospike nozzle in differential throttling configurations. A calibration of the thrust measurement system has been carried out.**

***Index Terms*—thrust measurement, aerospace nozzle, differential throttling**

## I. INTRODUCTION

The space exploration efforts of the 20th century were dominated by government agencies from the Soviet Union, the USA, and later the European Union. Over time, space technology transitioned to public-private partnerships, with the private sector recently entering Earth-to-orbit launch capabilities, exemplified by companies like United Launch Alliance and SpaceX. This shift has been supported by agencies like NASA, which encourage private sector innovation in space transportation. Today, the focus is on reducing launch costs and improving reliability, with private companies leading efforts in reusability, such as landing liquid-fueled rockets. While space exploration remains costly, advancements in science and engineering are making it more feasible.

One essential component of a launch vehicle and spacecraft is the propulsion system, and any improvements in propulsion performance contribute to the achievement of space exploration goals for humanity. A critical element of jet propulsion is the nozzle. Currently, both air-breathing jet engines and rocket engines mainly use conventional convergent-divergent nozzles, which have a limitation: they do not self-adapt to changes in ambient pressure, causing a loss of performance beyond their design point. This inherent weakness in the design of conventional nozzles has led scientists and engineers to explore innovative nozzle solutions, aimed at reducing mission costs and improving controllability.

Continued interest of space community in advanced nozzles encourage research community to characterize the static and dynamic behavior of these nozzles along with innovative thrust vector control strategies. A nozzle test rig was designed and manufactured at Politecnico di Torino (PoliTo), with the aim of establishing the groundwork for future research on advanced nozzles and their control strategies [10]–[12].

In this paper a linear aerospike nozzle has been utilized as test-case for measurement of the vectorized thrust obtained by differential throttling technique. Three precision balances positioned at the base of the test rig and arranged in a 120-degree configuration have been used to accurately reconstruct the thrust vector. The measured forces are compared with the results from numerical simulations conducted on the same nozzle model.

The aerospike nozzle chosen for this test is particularly interesting for aerospace propulsion and its self-adapting capability to ambient pressure. It adapts continuously with altitude up to design point. The linear aerospike configuration has been proposed for the propulsion system of the reusable launch vehicle (RLV) X-33 concept [1].

Aero vehicles likely require engine thrust vector control (TVC) for extra maneuverability and to maintain desired flight trajectories. Thrust vector control allows the alignment of the vehicle thrust with vehicle center of gravity to maintain straight line flight or to induce vehicle steering as desired. The conventional method of thrust vectoring involves mechanical means to deflect the direction of flow of the exhaust gases, whereas alternative method involves fluidic thrust vectoring (FTV) techniques. Fluid-based thrust vectoring has the advantages of simplicity and low weight over mechanical-based thrust vectoring, which adds to geometric complexity and extra weight to the vehicle [7]. FTV can be divided into following categories: shock vector, bypass shock vector, counterflow, coflow, throat skewing, dual throat, and bypass dual throat nozzle control [5]–[7], [9]. Ref. [7] concludes that bypass dual-throat nozzle control can achieve better thrust vectoring performance with large vector angles and low thrust loss.

Among other possibilities, differential throttling seems promising control technique in rocket engines. In a launch vehicle with multiple rocket engines, differential throttling will produce variable thrust in different combination of rocket engines which will result in desired orientation. Differential throttling is a simple control strategy which can be applied in

the presence of clustered aerospike engines with multiple independent combustion chambers or in linear aerospike engine where primary nozzles on either side of the plug will operate at different conditions. This asymmetry of inlet conditions generates a lateral thrust component which can be used for maneuvering [11].

## II. EXPERIMENTAL SETUP

### A. TEST RIG

A test rig has been designed at the Mechanical and Aerospace Department of PoliTo for cold-flow testing, as described in references [8, 9].

The test rig serves as a platform for mounting interchangeable test models. Its structure follows a tripod design with the upper section providing an attachment flange for the test model. The lower section connects to an intermediate piping system which includes a downstream conduit, a flow straightener, and a diffuser. The diffuser is linked to a corrugated metal flexible hose, whose free end can be connected to a pressurized air supply line. The inner nominal diameter of the flexible hose is 25.4 mm. The rig is designed to operate at a total pressure of 6.5 bar (6.42 atm). Fig.1 is showing a picture of the experimental test rig.

In this paper a linear aerospike nozzle has been utilized as test-case for measurement of the vectorized thrust obtained by differential throttling technique. Three precision balances positioned at the base of the test rig and arranged in a 120-degree configuration have been used to accurately reconstruct the thrust vector, (see Fig. 2). The balances have a full-scale range of 220 kg with a precision of 10 g. The minimum measurable weight is 30 g. They have four load cells positioned at the extremities, and they use a LCD display to facilitate the visualization of the measured weight.

### B. AEROSPIKE NOZZLE MODEL

A linear aerospike nozzles with 20% plug truncation (LASN-20) and nozzle throat width-to-height ratio of 30.41 has been utilized for the experimental and numerical tests. Dimensions of this nozzle are listed in table I.

This nozzle is shown in fig. 3. The nozzle has been designed for a nozzle pressure ratio, $NPR_D$, of 200, following the

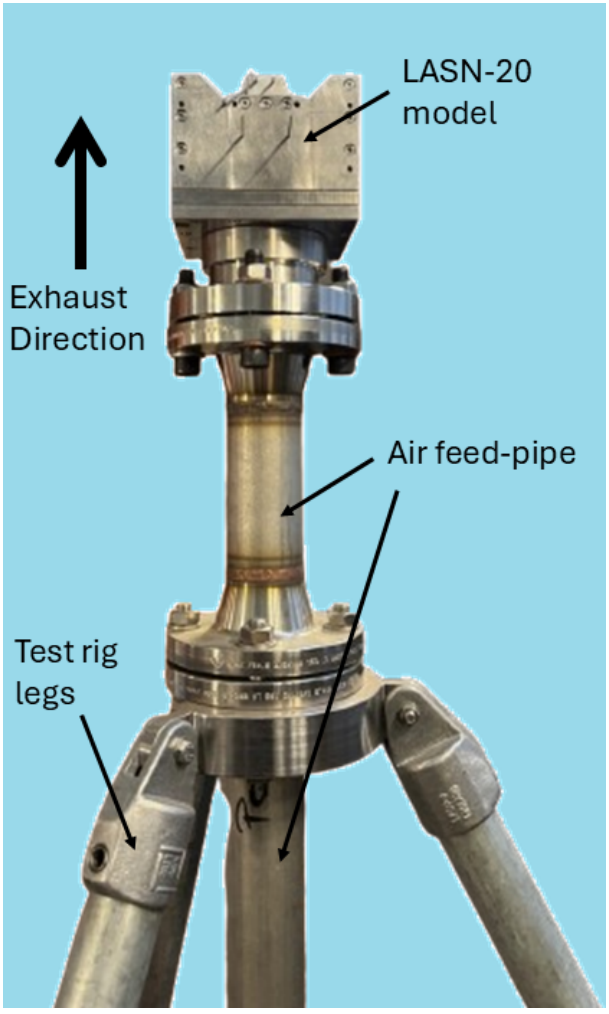



Fig. 1. Photo of upper part of test rig (with LASN-20 model installed at top)

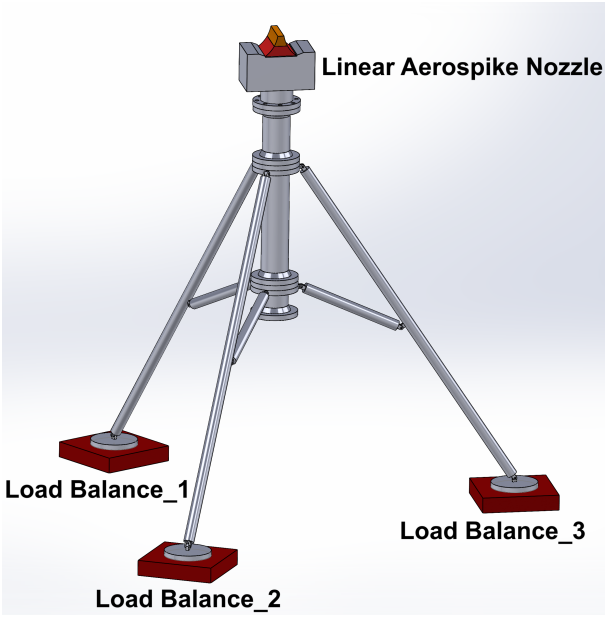



Fig. 2. Illustration of PoliTo test rig standing over 3 load balances, with linear aerospike nozzle installed at the top

TABLE I
NOZZLE DIMENSIONS

| | Symbol | Value |
|---|---|---|
| Aerospike Nozzle Exit Area | $A_e$ | $5003.21\,\mathrm{mm}^2$ |
| Width of Single Throat | $b$ | $77.55\,\mathrm{mm}$ |
| Height of Single Throat | $h_t$ | $2.55\,\mathrm{mm}$ |
| Area of Both Throats | $A_t$ | $395.51\,\mathrm{mm}^2$ |
| Width to Height Ratio, of the Throat | $b/h_t$ | 30.41 |
| Aeropspike Nozzle Area Ratio | $A_e/A_t$ | 12.65 |

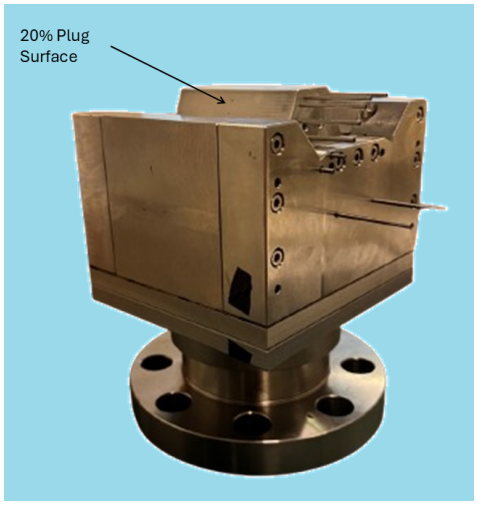



Fig. 3. Linear plug nozzle with $b/h_t$ = 30.41 and 20% plug truncation

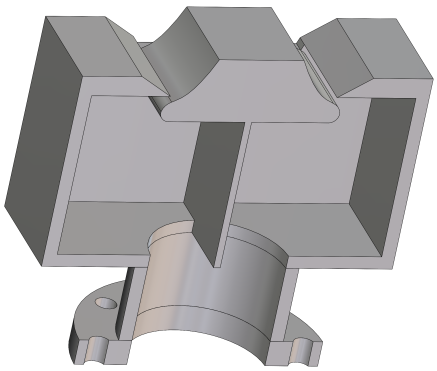


Fig. 4. Linear plug nozzle with two separated chambers (cutaway, not-to-scale)

guidelines described in [10]. Two separated chambers have been created in order to allow for differential throttling.

Since the nozzle is of a linear type, testing it in a differential throttling configuration requires delivering different mass flow rates to each of its chambers. This allows the two sub-nozzles to operate at different nozzle pressure ratios, (see Fig. 4).

To differentiate the flow rate in the two chambers, a throttling valve is provided at the inlet of one of the chambers. Three different throttling levels are achieved by varying the valve opening, as shown in Fig. 5. This produces a difference in the inlet area and, consequently, a different $NPR$ value between the upper ($NPR_T$) and lower ($NPR_B$) sub-nozzles. These two values are defining the differential factor $DF$ as:

$$DF(\%) = [1 - (NPR_T/NPR_B)] \cdot 100 \qquad (1)$$

### C. PRESSURE MEASUREMENT INSTRUMENTATION

The linear aerospike nozzle is equipped with eight orifices, 0.6 mm in diameter, located on one side of the plug surface

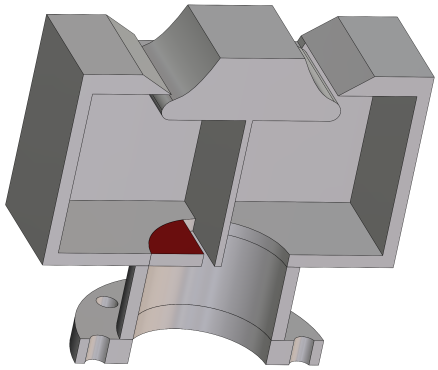


Fig. 5. Upper inlet restriction (in red) to reduce the mass flow rate (cutaway, not-to-scale)

along the symmetry-plane. These static pressure taps are shown in Fig. 6, with a spacing of 7 mm between each tap.

A DSA5000 pressure scanner of Scanivalve® [14] is used to measure the mean pressure distribution for both non-differential and differential throttling configurations.

The DSA5000 pressure scanner features a 16-channel architecture, with one pressure sensor per channel. It is capable of acquiring data streams at up to 5000 Hz (samples per channel per second). A unique aspect of this system is the use of an individual A/D converter for each sensor, enabling fully synchronous data collection. The system has a pressure range of 0 – 250 psi (0 – 17.01 atm) and offers a long-term accuracy of ±0.04% Full-Scale. It employs 24-bit A/D converters. Additional features can be found in reference [14].

## III. NUMERICAL SIMULATIONS

Numerical simulations, used in this paper for comparison with experimental data, have been carried out using commercial software of Ansys-Fluent. A two-dimensional domain has been used which is taken from symmetric plane of full geometry in Fig. 4, without inlet circular duct. The two-dimensional computational domain consists of a mesh with

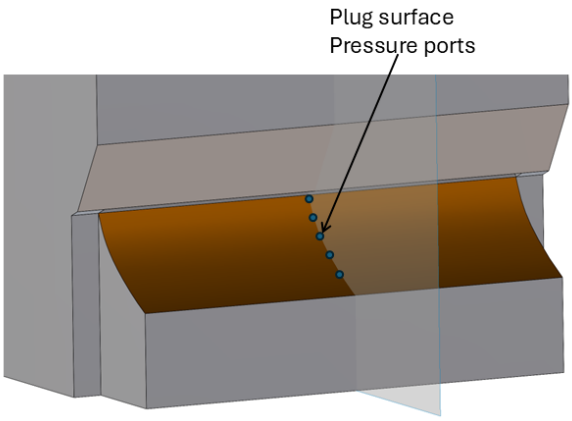



Fig. 6. Pressure taps on the nozzle plug wall

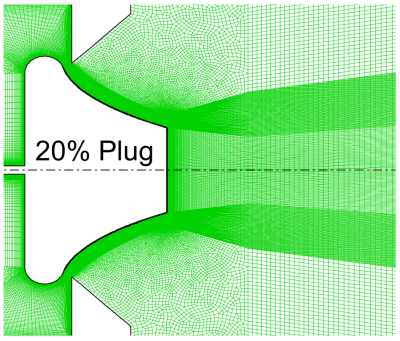



Fig. 7. Mesh of 2D computational domain

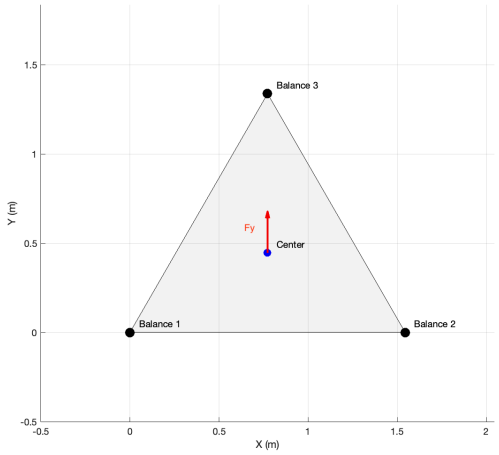



Fig. 8. Coordinates reference system and balance positions

$1.6 \times 10^5$ cells, as shown in Fig. 7. Numerical solutions were obtained using the steady-state, density-based solver in Ansys Fluent, which is based on the numerical integration of the RANS equations. The Spalart-Allmaras turbulence model was employed, and an implicit formulation with an AUSM flux scheme was used for the solution.

For unthrottled case, both sub-nozzles are set to the same nozzle pressure ratio of 4.0 ($NPR_T = NPR_B = 4.0$). For differential throttling cases, the top sub-nozzle is subjected to a reduce nozzle pressure ratio ($NPR_T$) compared to the $NPR_B$.

## IV. RESULTS AND DISCUSSION

In this section, 2D CFD data and current experimental results are presented and discussed.

In Fig. 9 and Fig. 10, experimental pressure data are presented alongside the corresponding numerical pressure distributions for $NPR_B = 2.8$ with $DF = 3.6\%$ and $NPR_B = 3.8$ with $DF = 10.5\%$, representing cases of differential throttling.

Thanks to the throttling valve, it is possible to modulate the $NPR_T$ of the top sub-nozzle. At the same time, the $NPR_B$ of the lower sub-nozzle remains unchanged.

It can be observed that as the $DF$ value increases (i.e., as $NPR_T$ decreases for a given $NPR_B$), the local peaks in the pressure distribution shift upstream toward the throat and decrease in intensity. The asymmetry in the pressure distributions between the upper and lower side walls of the linear plug generates a resultant side force, which leads to thrust vectoring. The experimental data align very well with the 2D CFD results. As seen in all these figures, the nozzle operates under overexpanded conditions, with the presence of compression and expansion waves.

As mentioned before, the purpose of this work is to validate the thrust values obtained from an aerospike nozzle using a numerical method with experimental measurements through balances appropriately positioned at the base of the test rig. The balances, being placed 120 degrees apart from each other, should be able to measure the axial and the transverse components of the thrust resulting from differential throttling. The figure 11 shows the normalized axial thrust component as a function of the expansion ratio (NPR), numerically calculated in the case of an unthrottled nozzle ($DF$=0%).

In Figures 12a and 12b the numerical results are shown in terms of axial force and normal force obtained on the nozzle as a function of the percentage of differential throttling ($DF$ varing from 0% to 50%.

A calibration of the thrust measurement system was carried out using precision balances placed at the base of the test rig. Weighing operations were performed by applying a vertical load and generating a moment with respect to the x-axis passing through two of the test rig feet. The $y$-axis is orthogonal to the $x$-axis, and passes through the center of balance 1, (see Figure 8). Consequently, the $z$-axis is oriented upward and coincides with the symmetry axis of the test rig. This approach was taken because the linear aerospike nozzle is oriented in such a way that any transverse thrust component is directed along the y-axis, thus generating only a moment $M_x$. The load tests performed yielded an accuracy of 1% for the measured vertical force component, $F_z$. The accuracy for the moment $M_x$ was approximately 10% of the measured value. In a second phase, the calibration is expected to involve the other components of the resulting moment as well.

## REFERENCES

[1] G. Hagemann, H. Immich, T. V. Nguyen, and G. E. Dumnov, "Advanced rocket nozzles," *Journal of Propulsion and Power*, vol. 14, no. 5, pp. 620–634, 1998.

[2] "The Linear Aerospike Engine," *From X-33 Prog OFC 8055725801, NASA*, pp.5-9, May 14, 1998. https://ntrs.nasa.gov/api/citations/19990004339/downloads/19990004339.pdf

[3] Marcello Onofri and et al, "Plug nozzles summary of flow features and engine performance," *RTO-TR-AVT-007-V1*, 2006.

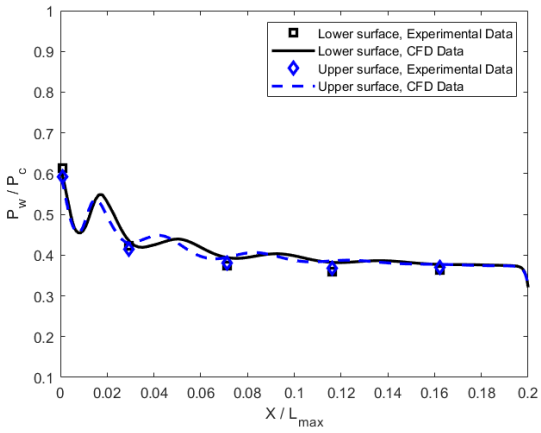



Fig. 9. $NPR_B = 2.8$, $NPR_T = 2.7$, $DF = 3.6\%$

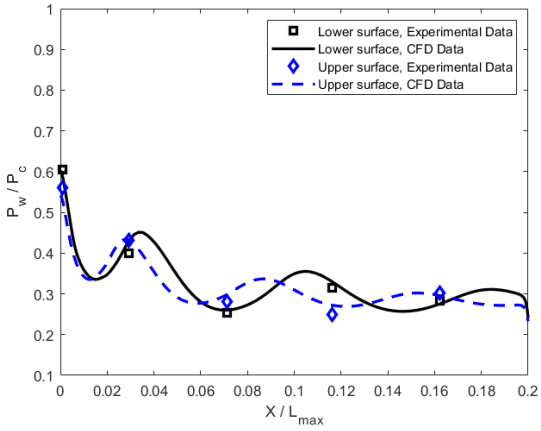



Fig. 10. $NPR_B = 3.8$, $NPR_T = 3.4$, $DF = 10.5\%$

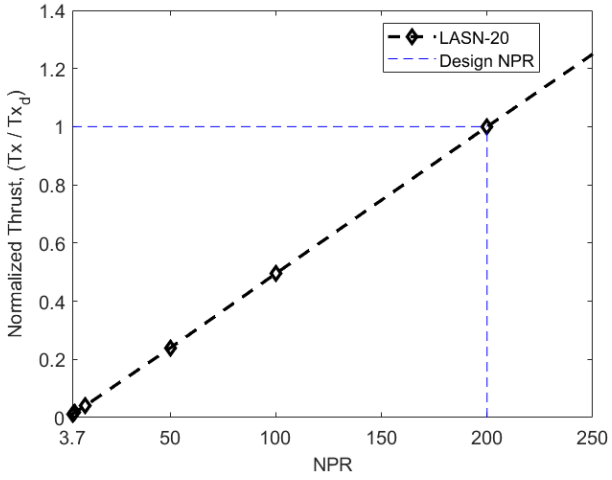
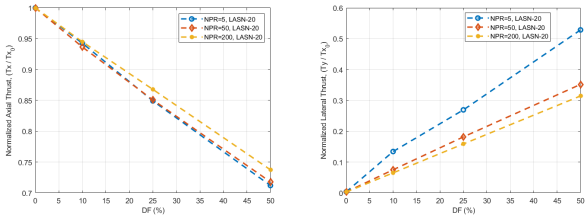



Fig. 11. Numerical Normalized Axial Thrust Component for $DF$=0




(a) (b)

Fig. 12. Numerical Thrust Components: a) axial component, b) normal component


[4] C. Warsop, and W. J. Crowther, "Fluidic Flow Control Effectors for Flight Control," *AIAA Journal*, 2018.

[5] K. Wu, H. Kim, "Theoretical and numerical studies on the performance of shock vector control," *ASME-JSME-KSME 8th Joint Fluids Engineering Conference*, 2019.

[6] Y.A. Sazonov, M. Mokhov, A. Bondarenko, V. Voronova, and K. Tumanyan, and E. Konyushkov, "Interdisciplinary studies of jet systems using Euler methodology and computational fluid dynamics technologies", *HighTech. Innov. J.*, 2023.

[7] Saadia Afridi, Tariq Amin Khan et al., "Techniques of Fluidic Thrust Vectoring in Jet Engine Nozzles: A Review," *Energies 2023, 16, 5721.*

[8] M. Ferlauto, R. Marsilio, "Open and closed-loop responses of a dual-throat nozzle during thrust vectoring", *AIAA Paper 2016-4504, 52nd AIAA/SAE/ASEE Joint Propulsion Conference, 2016.*

[9] M. Ferlauto, R. Marsilio, "A numerical method for the study of fluidic thrust vectoring", *Advances in Aircraft and Spacecraft Science, 3(4):367–378, 2016.*

[10] V. Bonnet, F. Ortone, G. M. D. Cicca, R. Marsilio, and M. Ferlauto, "Cold gas measurement system for linear aerospike nozzles," *9th International Workshop on Metrology for AeroSpace(MetroAeroSpace)*. IEEE, 2022.

[11] G. M. Di Cicca, J. Hassan, E. Resta, R. Marsilio, and M. Ferlauto, "Experimental characterization of a linear aerospike nozzle flow," *10th International Workshop on Metrology for AeroSpace(MetroAeroSpace)*. IEEE, 2023.

[12] G. M. Di Cicca, E. Resta, R. Marsilio, and M. Ferlauto, "A Framework for Testing Differential Throttling in Linear Aerospike Nozzle," *11th International Workshop on Metrology for AeroSpace(MetroAeroSpace)*. IEEE, 2024.

[13] G. Angelino, "Approximate method for plug nozzle design", *AIAA Journal*, vol. 2, no. 10, pp. 1834–1835, 1964.

[14] "DSA5000 Ethernet Pressure Scanner," *Scanivalve®*, https://scanivalve.com/products/pressure-measurement/ethernet-intelligent-pressure-scanners/dsa5000/